Impact of pore-water freshening on clays and the compressibility of hydrate-bearing reservoirs during production

J. Jang[1]*, S.C. Cao[2], W.F. Waite[1] and J. Jung[2,3]
[1] *U.S. Geological Survey, Woods Hole, MA, USA*
[2] *Louisiana State University, Dept. of Civil and Environ. Engineering, Baton Rouge, LA, USA*
[3] *Chungbuk National University, Dept. of Civil Engineering, Cheongju-si, Chungbuk, South Korea*
*Corresponding author: jjang@usgs.gov

Abstract

Gas production efficiency from natural hydrate-bearing sediments depends in part on geotechnical properties of fine-grained materials, which are ubiquitous even in sandy hydrate-bearing sediments. The responses of fine-grained material to pore fluid chemistry changes due to freshening during hydrate dissociation could alter critical sediment characteristics during gas production activities. We investigate the electrical sensitivity of fine grains to pore fluid freshening and the implications of freshening on sediment compression and recompression parameters.

Introduction

Natural methane hydrate in offshore and onshore sediments is considered a potential energy resource, with the international gas hydrate community planning a number of offshore and onshore production tests to examine the logistical requirements and economic realities of extracting methane from hydrates [1-5]. Although favorable targets for gas production from hydrate-bearing sediments are coarse-grained sediments with high-hydrate concentrations [6], fine-grained materials ("fines") are mixed in with these sediments dominated by coarse-grained sands, and may additionally form reservoir interbeds and seal layers that are fines-dominated. These fines are likely to impact the overall sediment formation response and production efficiency during gas production [3, 7]. A key consideration is sediment compressibility, with low compressibility being desired for maintaining sediment structure and preserving permeable pathways to a production well. This study focuses on compressibility changes due to fines responding to the pore-water freshening that occurs as hydrate dissociates in situ.

Fine-grained material refers mainly to silts and clays, which have characteristic particle sizes less than 75μm [8]. The plasticity index, which distinguishes silts from clays, represents the water content range required to transition from a liquid state to a semi-solid state and is related to interactions among particles and pore water [8]. Clays, which have a high plasticity index, are more pliable in their plastic states due primarily to electrical interactions among the particles and pore fluid. Clay particles often possess excess or unbalanced electrical charges on their surface due to isomorphous substitution, surface dissociation of hydroxyl ions, absence of cations in the crystal lattice, structural disorder and defects [9, 10]. In conjunction with their small particle size, the unbalanced surface charge can make fines susceptible to electrical interactions that control the arrangement or "fabric" of collected particles [11, 12].

The primary attractive and repulsive forces relevant to the particle interactions in this study are shown in Figure 1. The Sogami-Ise model in Figure 1(a) describes attractive and repulsive electrical interactions among particles with net surface charges [13, 14]. For example, when particles such as montmorillonite are in water, the net surface charge of each particle can push like-charged particles away as shown in Figure 1(a)-deionized water. This behavior can also be called diffusive double layer, DDL, repulsion. The repulsion separates particles and can build a dispersed fabric with a relatively large void ratio. However, counter ions present in the fluid, such as those that exist in a brine, adsorb onto the charged surface, decreasing the electrostatic repulsion between particles. In spite of the reduced electrical field around the particles, counter ions remaining in the pore fluid continue to be attracted to the spaces between particles and provide an attractive electrical interaction that leads particles to flocculate and form face-to-face fabrics with lower void ratios than occur in deionized water (Figure 1(a)-brine).

Electrical interactions due to localized surface charges on particles can also affect how the particles arrange themselves to form the sediment fabric [9, 10]. For example, when platy particles such as kaolinite or muscovite are immersed in deionized water, positively-charged particle edges are attracted to the negatively-charged faces of neighboring particles: the attractive electrical interaction forms the edge-to-face, high void ratio fabric of platy particles (Figure 1(b)-deionized water). If these particles are immersed in a brine instead of deionized water, counter ions in the fluid can surround the particles, reducing the edge-to-face attractions. The counterions provide an attractive force that makes platy-like particles more prone to relatively low void, parallel particle arrangements as shown in Figure 1(b)-brine.

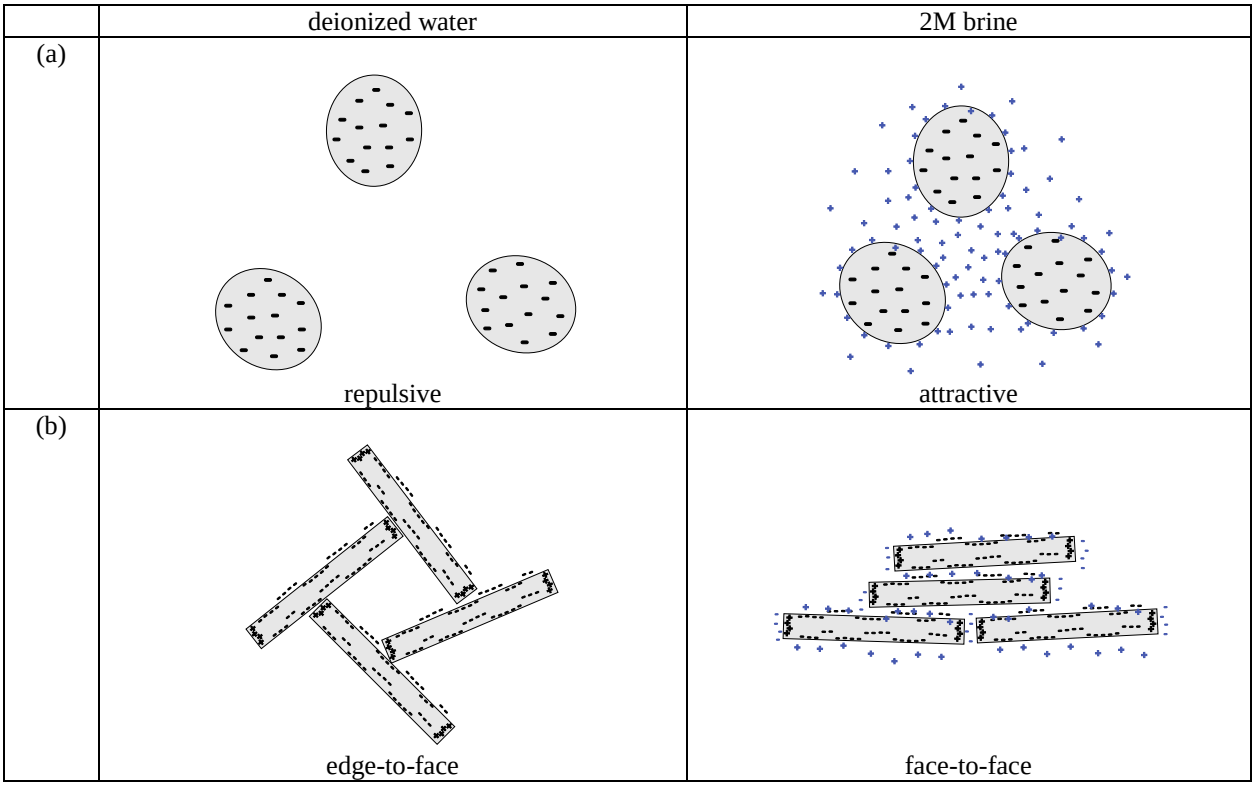

Figure 1: Mechanisms of electrical interactions among particles. (a) Sogami-Ise model – repulsive and attractive interaction due to net excess surface charge interactions [13, 14]. (b) Attractive interactions due to localized excess surface charge: edge-to-face fabric (deionized water) and face-to-face fabric (brine). Transition from fabrics seen in deionized water to those seen brine generally occurs between 0.01M and 0.1M, depending on surface charge conditions [10, 12].

As suggested in Figure 1, strength of the attractive and repulsive electrical forces discussed here are influenced by pore water chemistry changes. Both forces are disrupted by increased ionic concentrations, c_0 [mol/L]. For instance, the DDL thickness, ϑ, expands and shrinks based on c_0 and the relative permittivity of the pore-fluid, κ', according to [10, 12, 15]:

$$\vartheta \propto \sqrt{\frac{\kappa'}{c_0}}. \qquad \text{Eq. 1}$$

Changes in these micro-scale interactions alter the sediment fabric during deposition or sedimentation [9, 16-18] but pore-water chemistry changes can also have macroscopic impacts on in situ sediment properties such as strength and compressibility [19-22]. For example, the freshening of marine sediment pore water (e.g., during hydrate dissociation or submarine groundwater flow) can induce swelling (increased DDL thickness) between fines and trigger marine slides [23]. Pore-water freshening is an important byproduct of gas production from hydrate-bearing sediment. Dissociating a unit volume of methane hydrate produces 0.79 volumes of pure water, meaning the dissociation of uniformly-distributed hydrates in $1m^3$ of hydrate-bearing sediment with 45% porosity and 80%

hydrate saturation would mix 0.284m^3 of fresh water into the existing 0.09m^3 of pore fluid brine, reducing the salt concentration to 25% of the original salt concentration. Depending on the hydrate distribution, local salt concentrations could become low enough to alter particle interactions, particle arrangements, and sediment compressibility.

Understanding the macroscopic impact of pore fluid changes on sediment compressibility is particularly important because pilot tests for gas production from hydrate-bearing sediments mainly use the depressurization method [1-5], which increases the effective stress that governs sediment compaction [24]. Predicting how a reservoir unit compacts in response to an effective stress increase during depressurization requires incorporating how the reaction of fines to the ongoing pore water freshening alters the formation compressibility. This study uses the electrical sensitivity of fine grains [25] to link pore fluid chemistry changes to alterations in fabric formation and compressibility of a diverse suite of endmember soils.

Experimental Methods

Three types of experiments are described here. Electrical sensitivity studies, based on the approach of *Jang and Santamarina* [25], are used to classify the endmember fines in this study. Sedimentation tests are then run on the endmember fines using a range of pore water salinities to provide insights into the interparticle forces relevant to each endmember sediment. Finally, consolidation tests are run for each endmember sediment using deionized water and then, separately, brine to quantify the impact of pore water salinity on compressibility. These compressibility results are analyzed in light of the electrical sensitivity classification of each sediment and the particle behavior observed in the sedimentation tests.

Materials

We selected endmember, pure fines to illustrate the effect of pore-fluid freshening over a range of electrical sensitivities, shapes, sizes and chemical compositions. The chosen sediments were silica silt, mica (muscovite), calcium carbonate ($CaCO_3$), diatom, kaolin (primarily made of kaolinite), and bentonite (primarily made of montmorillonite) (Table 1). Of these, silt-size quartz, mica, kaolinite and smectite (the clay group that includes montmorillonite) are common in onshore and offshore sediments, while diatoms and organic calcium carbonate in the form of microfossils are frequently found in marine sediments [4, 26-28]. The pore fluids used in this study were deionized water (DW), sodium chloride (NaCl) brines with 0.001M, 0.01M, 0.1M, 0.6M and 2M NaCl concentrations, and kerosene. The 0.6M salt solution (~35 parts per thousand) was chosen as being typical of marine pore fluids, and kerosene is a low permittivity fluid required for characterizing electrical sensitivity [25]. The fluid pH at the beginning of each test was 7.

Electrical Sensitivity

A soil's electrical sensitivity is defined in terms of its liquid limit measured for deionized water, 2M brine and kerosene [25]. Liquid limits, measured using a cone penetrometer [29], indicate the water content for which a sediment transitions from a semi-solid to a liquid state. In addition to informing the electrical sensitivity characterization, liquid limits are related to other physical properties of remolded soils such as hydraulic conductivity and compressibility [30-33]. We performed the cone penetrometer-based electrical sensitivity tests on each sediment to assess alterations in electrical interactions between fines in response to the fluid's permittivity, κ', and conductivity [25], which itself is related to the ionic concentration, c_0 (details in [25] of the reference list).

Sedimentation Test

Sedimentation tests were run for different pore fluids to provide insights into how interparticle arrangements (sediment fabric) and particle segregation depend on pore fluid chemistry [17, 18]. Beginning with oven-dried specimens, we measured out the sediment weight required to create a loose-packed (maximum void ratio) fabric to a height and diameter of 25.4 mm in an acrylic mold by placing the material in the mold using a spoon. The soil specimen was then mixed with fluid to a final height of 152.4 mm (six times the original sediment height) using one of six fluids: deionized water, 0.001M, 0.01M, 0.1M, 0.6M, or 2M brine. The mixture was allowed to stabilize for more than 12 hours. The fluid in the cylinder was vacuumed in order to remove air, and then the cylinder was shaken for one minute before being left to settle undisturbed. Heights of the depositional interface and the accumulated sediment interface defined in Figure 2 were measured as a function of time until the interface locations stabilized (1 to 4 days).

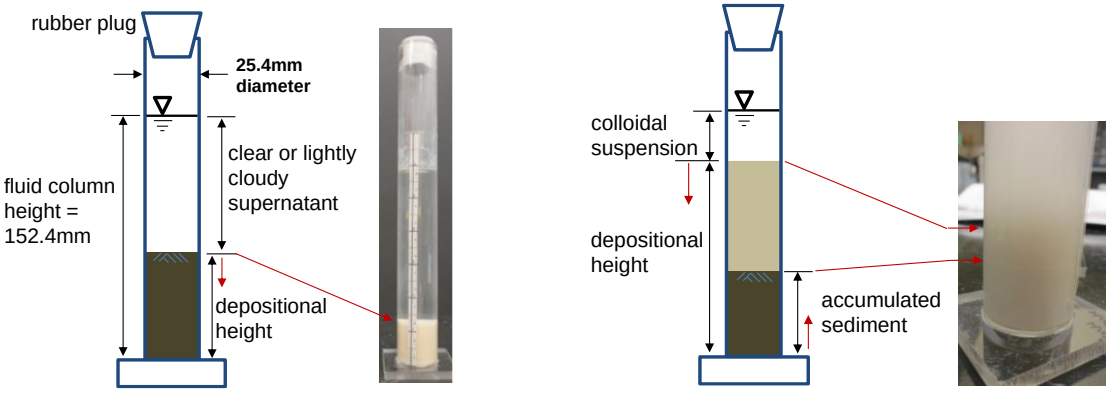

Figure 2: Height measurements observed in sedimentation tests: (a) a uniform sedimentation response in which essentially all sediment particles fell together such that a sharp interface was observed at the depositional height between the sediment and overlying clear or lightly cloudy supernatant; (b) a segregated sedimentation response in which the sediment segregated (due to different falling velocities of individually-sized particles) into a bottom layer containing the largest particles (accumulated sediment), a middle layer extending to the depositional height and containing smaller particles, and an overlying cloudy colloidal suspension containing the finest particles [17].

Consolidation Test

We conducted incremental loading consolidation tests in a 1-dimensional fixed-ring oedometer cell as described in [34] to evaluate the compressibility of end member sediment in each pore fluid. The fluid content of the specimen for each consolidation was 1.2LL, where the liquid limit, LL, was determined from the cone penetrometer tests. The specimen was mixed with pore fluid (deionized water or 2M brine) and stabilized overnight before being placed in a rigid consolidation ring of 25.4mm height and 63.5mm diameter. The specimen was fully submerged during the consolidation test.

Experimental Results and Discussion

Table 1 shows the endmember soil material properties. The selected soils cover a wide range of material properties, physical morphologies and chemical compositions.

Table 1: Material description: physical and index properties

No.	soils	median particle size[1] D_{50} [µm]	specific surface S_s [m^2/g][2]	liquid limit[3]			electrical sensitivity soil classification[4]	sedimentation test - dry weight at loose [g][5]
				LL_{DW}	LL_{brine}	LL_{ker}		
1	silica silt	10.5[1]	0.2[6]	31	31	36	LI	9.13
2	mica	17[1]	4.2	94	81	110	HI	3.59
3	$CaCO_3$	8[1]	0.2[6]	25	23	31	NI	9.87
4	diatoms	10[1]	98	119	111	140	HI	2.90
5	kaolin	4	24	77	55	83	II	5.57
6	bentonite	< 2[7]	579	288	126	65	HH	9.71

[1] data from manufacturer
[2] water-based methylene blue test [35]
[3] following the approach of [25], liquid limit is corrected to compare the results to the liquid limit with deionized water
[4] indicating no (N), low (L), intermediate (I), or high (H) plasticity fine grains of low (L), intermediate (I), or high (H) electrical sensitivity in Figure 3
[5] sample mold size: 25.4 mm in diameter and height
[6] analytical calculation based on spherical particle shape
[7] approximated value from literature [36]

Figure 3 plots their electrical sensitivity. Silica silt, $CaCO_3$, diatoms and mica are considered to have an intermediate electrical sensitivity because of their sensitivity to electrical permittivity changes, but as indicated by similarities between the deionized water (DW) and brine liquid limit values in Table 1, these four sediments show a smaller sensitivity to ionic concentration, c_0 (brine), than to permittivity, κ' (kerosene). Because of its small particle size and large excess surface charge, bentonite is strongly influenced by the diffuse double layer thickness, which via Eq. 1, responds to both c_0 and κ' changes in the pore-fluid chemistry. Correspondingly, bentonite has the highest electrical sensitivity of the tested sediments (Figure 3).

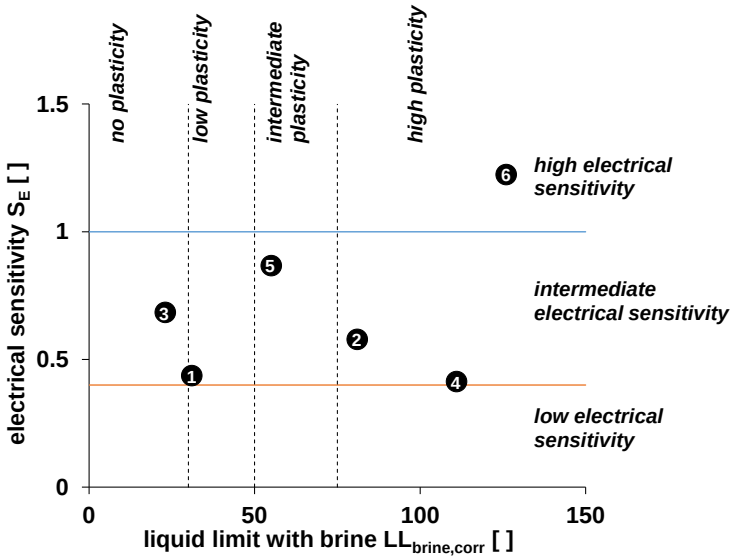

Figure 3: Chart for soil classification based on electrical sensitivity. Numbered black circles refer to the sediments in Table 1.

Sedimentation Tests

Figure 4 shows the sedimentation test results for both the uniform and segregated sedimentation described in Figure 2. Kaolin and bentonite (Figure 4a and b) both demonstrate a uniform settlement pattern. In the case of kaolin, particles flocculate as shown in Figure 1(b)-DW when the ionic concentration is low, and the flocculated clusters can settle relatively rapidly. As ionic concentration increases toward the 2M brine, the electrical interaction for edge-to-face clustering are weakened or shielded by the added ions in the water. The platy kaolinite particles in the kaolin begin to cluster in face-to-face mode as shown in Figure 1(b)-brine. These parallel clusters develop more slowly than the edge-to-face clusters [18], as demonstrated by the increased settling times for higher brine concentrations.

In the case of the highly electrically-sensitive bentonite (Figure 4b), electrical repulsive interactions are so strong in deionized water that bentonite particles cannot pack or settle, and the depositional interface does not fall (Figure 4b, inset, left). Only after the addition of 0.6M NaCl is the ionic concentration driven high enough (Eq. 1) for particles to settle, albeit slowly. Additional increases in ionic concentration further shrink the DDL thickness, allowing bentonite particles to approach close enough to each other to begin clustering and settling more rapidly. Once settled, they also pack more efficiently (attain a lower depositional height) when the DDL thickness is small.

In segregated sedimentation (defined in Figure 2b; Figure 4c, d), the accumulated sediment and depositional interfaces are not as clearly defined as the depositional interface is in uniform sedimentation. When silica particles are of uniform grain size, they exhibit uniform sedimentation [38], but the specimens tested here contain grain size ranges that span two controlling factors for sedimentation. Larger particles fall gravimetrically without being influenced by the electrical interactions (Figure 1a) that exert significant controls on the sedimentation of smaller particles in the specimen. This sedimentation behavior provides a mixed pattern of the electrical interactions introduced in Figure 1. While the larger particles are falling gravimetrically, the smaller silica silt particles form diffusive double layers near their surfaces [37] and remain suspended. Though these DDL are not nearly so prominent as they are in the highly-electrically-charged bentonite case, the small particles in the cloudy supernatant above the accumulated sediment interface behave similarly to the falling pattern of bentonite. Increasing the salt

concentration adds more ions, which allows a greater fraction of the small particles to cluster (Fig. 1a-brine) and settle. This enhanced clustering with increased brine concentration increases the falling velocity of the depositional interface and also more quickly clears up the supernatant liquid above the depositional interface. As more particles are involved in settling with increased brine concentration, the rise velocity and overall height of the accumulation interface also increase (Figure 4c). Because the DDL for silica is small compared to those of bentonite, the change in depositional rate with increasing brine content is not as significant for silica as that observed for bentonite (Figure 4b, d).

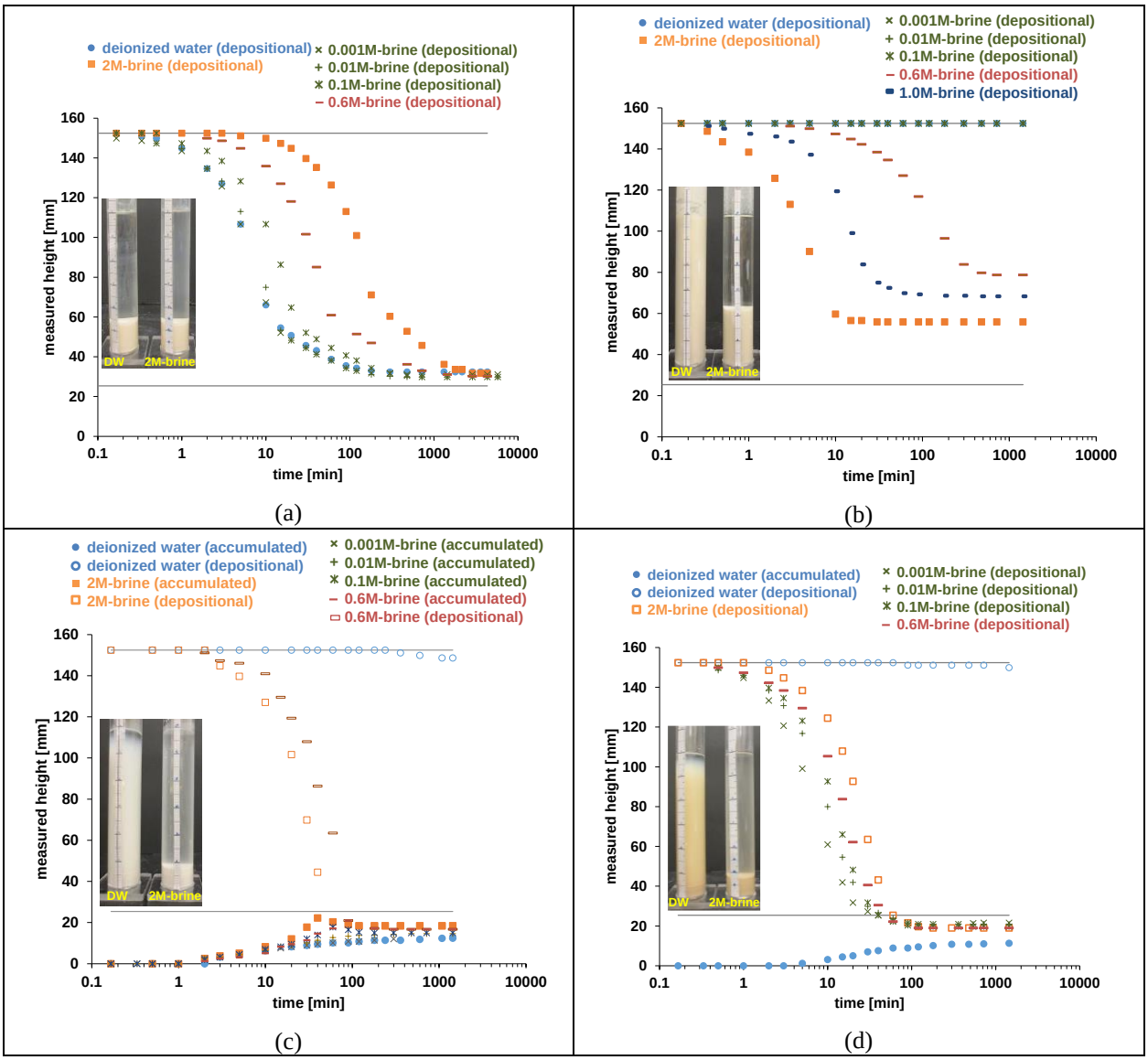

Figure. 4: Sedimentation interface height dependence on time. Black reference lines represent 152.4mm, the fluid column height; and 25.4mm, the initial height of each dry, loose-packed specimen. Symbol legends are given in each plot, and heights refer to the interfaces described in Figure 2. Inset images show examples of each specimen in deionized water (DW) and 2M brine. Upper row: (a) kaolin and (b) bentonite both demonstrate uniform sedimentation. Lower row: (c) silica silt and (d) mica both demonstrate segregated sedimentation.

The behavior of the smaller mica particles in the cloudy supernatant above the depositional interface in various brine solutions is akin to that of silica silt. The remnant above the depositional interface fades faster in high ionic concentration brine. However, the depositional interface falls more slowly as ionic concentration increases, and that

is similar to the observed behavior of kaolin. As with kaolin, an increase in ion concentration slows the falling velocity of platy mica (Figure 4d) because the electrical interaction time for face-to-face clustering is longer than that of edge-to-face clustering (Figure 1a).

Figure 5 shows the variation in sedimentation response to the highest and lowest ionic concentrations (2M brine and deionized water, respectively). The accumulated sediment heights for the lower sensitivity sediments (diatom, silica silt, mica) in deionized water are all less than their initial 25.4 mm height when dry (Figure 5a), indicating that segregated sedimentation separates fines into the colloidal suspension, leaving only the larger particles to contribute to the accumulated sediment height via gravity-dominated packing. The presence of brine (orange squares in Figure 5a) reduces the fraction of these specimens that remains suspended. Consequently, the accumulated settlement heights account for more of the original material, and are thus higher than what is measured in deionized water. That the fines fraction of even a low-electrical sensitivity sediment responds to pore fluid chemistry changes becomes an important insight for the consolidation test results.

The rate of interface movement (Figure 5b) is not a strong function of ionic concentration except for the most electrically-sensitive soils (kaolin and bentonite). As anticipated from the brine dependence of sedimentation shown in Figure 4a and b, brine causes kaolin to settle more slowly, and bentonite to settle more quickly, than in deionized water. In this case, the electrical sensitivity index only indicates which sediments will behave significantly differently in deionized water versus brine, and does not capture the sign of that dependence.

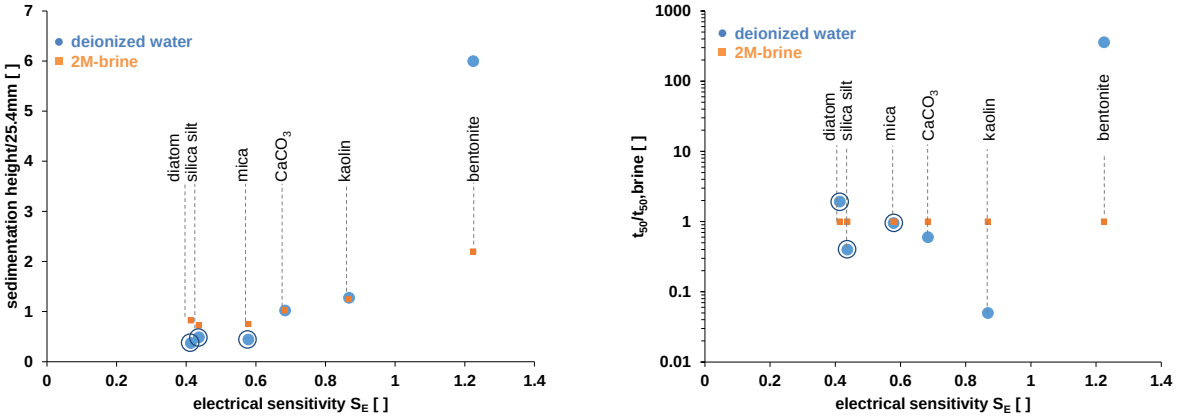

Figure 5: Sedimentation dependence on electrical sensitivity: (a) Ratio of final depositional interface height to initial dry height (25.4mm) and (b) Ratio of falling-time, t_{50}, when the measurable interface moves half its total travel distance relative to that in 2M brine. Because cloudiness obscured the change, if any, in the depositional interface height for silica silt, mica, and diatoms in deionized water (ringed blue circles), the accumulated sediment interface is used instead of the depositional interface. Rate measurements (b) suggest sediments with high electrical sensitivity will settle at dramatically different rates if disturbed during pore-water freshening, but whether the rate increases or decreases depends on the relevant electrical interaction for fabric formation.

Consolidation Tests

Figure 6 shows how the consolidation results for mica and kaolin depend on ionic concentration. The compression indices from consolidation tests are calculated from the slope of the compression curve during the initial compression, C_c, and during recompression, C_r, and represent the change in void ratio caused by changes in effective stress. The compression index, C_c, and recompression index, C_r, are calculated from Eq. 2 and presented in Table 2:

$$C_c \text{ or } C_r = \frac{e_{100kPa} - e_{1,000kPa}}{\log_{10}\left(\frac{1,000kPa}{100kPa}\right)} = e_{100kPa} - e_{1,000kPa} \qquad \text{Eq. 2}$$

where e_{100kPa} and $e_{1000kPa}$ are the void ratios at 100kPa and at 1,000kPa vertical effective stress, respectively.

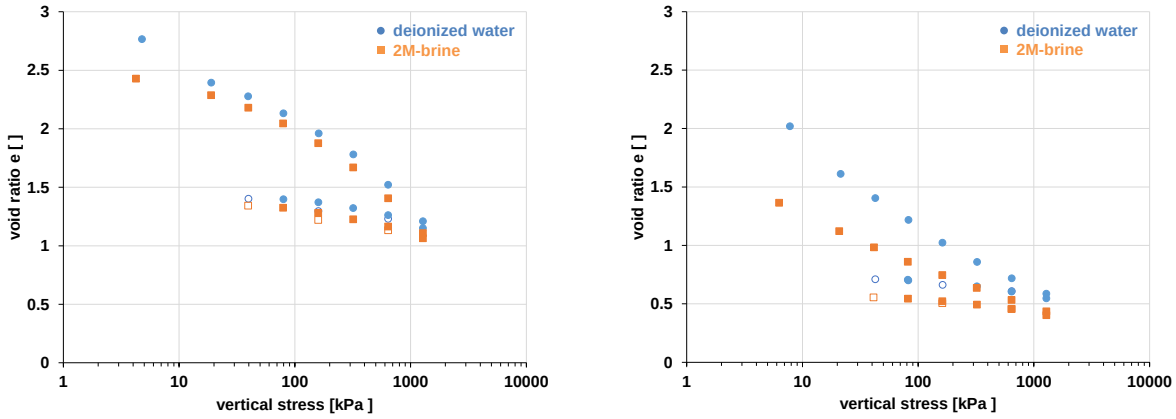

(a) (b)

Figure 6: Consolidation results for (a) mica and (b) kaolin

Table 2. Compression and recompression indices of endmember fine grains

No.	soils	compression index *Cc*		recompression index *Cr*	
		deionized water	2M brine	deionized water	2M brine
1	silica silt	0.08	0.1	0.03	0.03
2	mica	0.74	0.78	0.18	0.19
3	$CaCO_3$	0.1	0.09	0.018	0.012
4	diatom	0.385	0.56	0.105	0.12
5	kaolin	0.5	0.36	0.11	0.11
7	bentonite	2.8	1.02	1.61	0.26

The compressibility index dependence on electrical sensitivity is shown in Figure 7, normalized to the results in deionized water. In 2M brine, the compressibility scales with the electrical sensitivity, including transitioning from low-sensitivity materials being more compressible in brine to high-sensitivity materials that are much less compressible in brine. In low electrical sensitivity materials, the segregated sedimentation results (Figure 4c and d) are relevant. In deionized water, the finer particles that remain in suspension (Figure 2b photo, 4c and d) prefer to remain in the pore fluid in the compression test specimen, floating in the free pore space without interacting with the larger particles (Figure 8a). When the pore fluid is 2M brine, however, finer particles should be expected to settle along with the larger particles, coexisting at contacts between large grains as well as elsewhere in the pore space (Figure 8b). Thus, the fabric in brine is more easily compressed and has a higher compressibility index [39, 40]. The recompression index response to brine is similar to that of the compression index, with a notable exception for kaolin (discussed below). The recompression index in low electrical sensitivity soils changes only slightly between deionized water and brine.

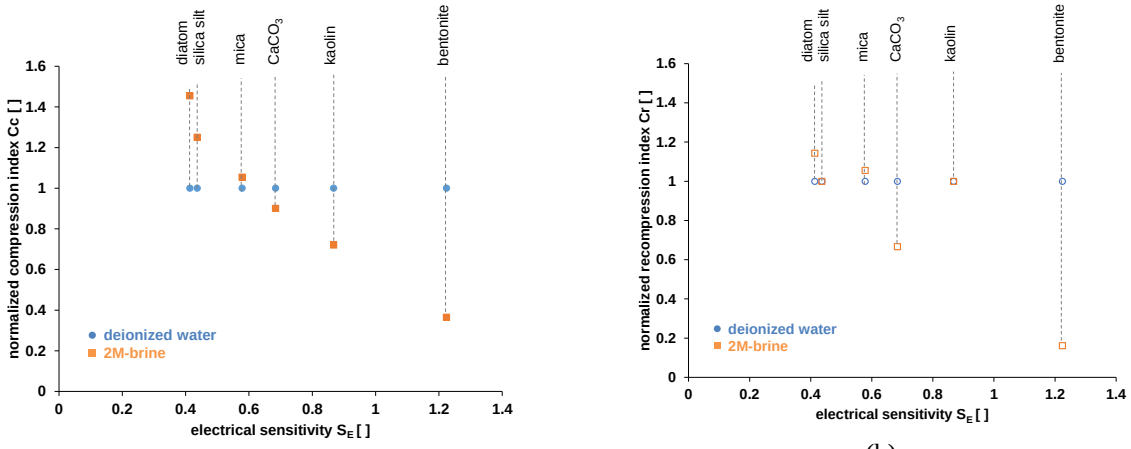

(a) (b)

Figure 7: Dependence of the (a) compression, C_c, and (b) recompression, C_r, indices on electrical sensitivity. Note the indices are normalized to their values for deionized water

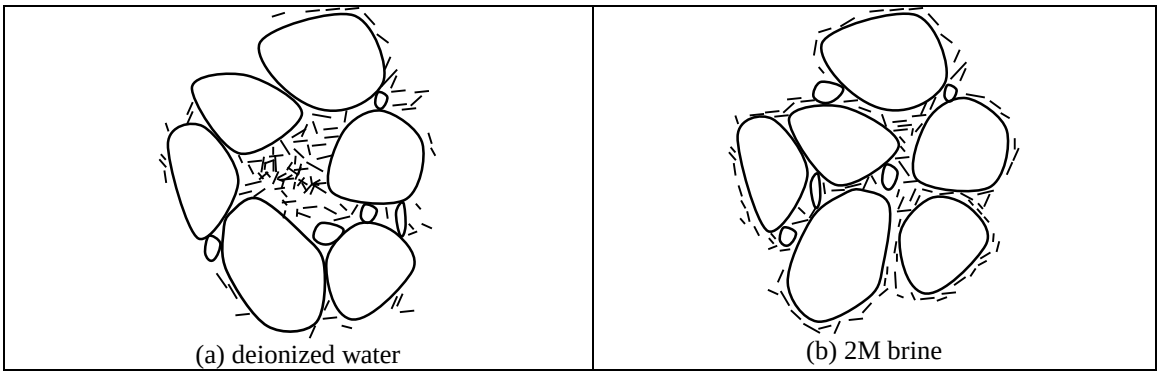

Figure 8: Effect of segregation in particle location. (a) When relatively small particles (bars) are held in suspension by electrical repulsion in deionized water, they can collect away from the contacts between larger grains. This arrangement is less compressible than (b), a more uniform distribution of small and large particles in which particles of all sizes are present at grain contacts and can be load-bearing participants of sediment deformation [39, 40].

Implications for hydrate-bearing reservoirs during production

The depressurization of a primarily coarse-grained hydrate-bearing formation increases effective stress while freshening pore water via hydrate dissociation. In hydrate-bearing sands with a fine fraction, these processes can be expected to disturb fines and alter sediment fabric in a manner similar to that observed for segregated sedimentation in systems with broad grain size ranges (Figure 4c,d). Fines might be expected to become suspended as fluid flow toward the production well commences and pore water is freshened. If those fines are electrically sensitive, they could remain suspended in the pore space away from the larger grain contacts. As depressurization continues and the effective stress increases, additional sediment compression could occur. The sediment's original compressibility in brine would transition toward its lower compressibility in deionized water as seen in Figure 7 for specimens that demonstrate segregated sedimentation.

In high electrical sensitivity sediments, increased ionic concentrations cause sediment to pack more densely based on fabric and DDL thickness (Figure 1 and 5a). Because the presence of brine causes the sediment to pack more densely initially, the specimen is less compressible than specimens with the very loose packing characteristic of highly electrically sensitive sediments in deionized water (Figure 7a). In a hydrate-bearing reservoir undergoing depressurization, pore water freshening could disturb electrically sensitive fines not already under an effective stress, causing them to transition to looser (higher void ratio) fabrics that would be more susceptible to subsequent compression.

In a hydrate-bearing reservoir, the recompression index is relevant when the reservoir is temporarily shut in. The reservoir pore pressure has a chance to recover during a shut in, reducing the effective stress. In sediments containing sediments governed by DDL repulsion, such as bentonite, a decrease in effective stress can allow the presence of freshened water to increase the DDL thickness, increase interparticle separation, and create a looser, more compressible sediment fabric. In the case of compacted kaolin, which is governed only by attractive forces, there is no drive for repulsion or swelling [41] (unless the kaolin is mechanically disturbed such as by high fluid-flow rates toward a production well), so no expansion is anticipated and thus the recompression and compression indices should be nearly equal (Figure 7b).

Conclusions

We investigate the responses of fine particles to pore water chemistry and stress state changes to provide a better understanding how these fines, which exist even in primarily coarse-grained hydrate-bearing reservoirs, behave during a possible gas production scenario in which induced depressurization leads to pore water freshening and an effective stress increase. We use electrical sensitivity measurements, a set of sedimentation tests and consolidation tests in fluids with a range of ionic concentrations to evaluate the dependence of sediment compressibility on pore water chemistry. We observe effects of pore-fluid chemistry on soil behavior, and present results in terms of the

soil's electrical sensitivity. Overall, the compressibility of the more electrically sensitive soils is more strongly influenced by changes in pore-fluid ionic concentrations. The following conclusions can be made:

1) Segregated versus uniform sedimentation – Fines migration: Even sediments with low electrical sensitivity, such as diatoms, silica silt and mica, can include a particle size fraction that is small enough to be significantly influenced by electrical forces. In a formation disturbed by the flow of freshened water toward a production well, electrical repulsion can hinder resettlement by the smaller particle size fraction, causing segregation in which intergranular contacts are dominated by the larger grains, with smaller grains left to float in the pore space.

2) Electrical interaction controls on fabric and compressibility: Pore fluid chemistry affects the depositional behavior and the compressibility of in situ sediment. Sediments containing coarser, gravimetrically controlled particles mixed with finer, electrically controlled particles would initially form more compressible fabrics in brine than in freshwater. During depressurization-induced pore water freshening, sediment with low electrical sensitivity would maintain the fabric, although the segregated colloids would be disturbed as discussed in (1) and the overall sediment compressibility would decrease as a result. Electrically sensitive sediments of interbeds such as bentonite or kaolin (if mechanically disturbed), would take up water and rearrange particles into a looser (higher void ratio) fabric owing to electrical interactions in freshened water. Fabric rearranged in this way is more susceptible to recompression.

Acknowledgements

This work was supported by the U.S. Geological Survey's Gas Hydrates Project, by an interagency agreement between the U.S. Geological Survey and the Department of Energy (DE-FE0023495), and by a Department of Energy grant awarded to Louisiana State University (DE-FE00-28966). This report was prepared as an account of work sponsored by an agency of the United States Government. Reference herein to any specific commercial product, process, or service by trade name, trademark, manufacturer, or otherwise does not necessarily constitute or imply its endorsement, recommendation, or favoring by the United States Government or any agency thereof.

References

[1] H. Takahashi, T. Yonezawa, E. Fercho. "Operation overview of the 2002 Mallik gas hydrate production research well program at the Mackenzie Delta in the Canadian Artic" *Offshore Technology Conference*, (2003) OTC 15124

[2] M. Kurihara, A. Sato, K. Funatsu, H. Ouchi, K. Yamamoto, M. Numasawa, T. Ebinuma, H. Narita, Y. Masuda, S. R. Dallimore, F. Wright, D. Ashford. "Analysis of production data for 2007/2008 Mallik gas hydrate production tests in Canada" *The Society of Petroleum Engineering*, (2010) SPE 132155

[3] B. Anderson, S. Hancock, S. Wilson, C. Enger, T. Collett, R. Boswell, R. Hunter. "Formation pressure testing at the Mount Elbert Gas Hydrate Stratigraphic Test Well, Alaska North Slope: Operational summary, history matching, and interpretations" *Marine and Petroleum Geology*, 28 (2011) 478-492

[4] B. Anderson, R. Boswell, T. S. Collett, H. Farrell, S. Ohtsuki, M. White, M. Zyrianova. "Review of the findings of the Ignik Sikumi CO2-CH4 gas hydrate exchange field trial" *Proceedings of the 8th International Conference on Gas Hydrates*, United States: China Geological Survey, Beijing, China (2014)

[5] K. Yamamoto. "Overview and introduction: Pressure core-sampling and analyses in the 2012-2013 MH21 offshore test of gas production from methane hydrates in the eastern Nankai Trough" *Marine and Petroleum Geology*, 66 (2015) 296-309

[6] R. Boswell, T. S. Collett. "Current perspectives on gas hydrate resources" *Energy & Environmental Science*, 4 (2011) 1206-1215

[7] R. Boswell, G. Moridis, M. Reagan. "Gas hydrate accumulation types and their application to numerical simulation" *Proceedings of the 7th International Conference on Gas Hydrate (ICGH)*, Manuscript 130 (2011) 17-22

[8] ASTM. (2011) *Standard Practice for Classification of Soils for Engineering Purposes (Unifined Soil Classification System).* ASTM D4318, West Conshohocken, PA

[9] T. W. Lambe, R. V. Whitman. *Soil Mechanics*. John Wiley & Sons(1969)

[10] J. C. Santamarina, K. A. Klein, M. A. Fam. *Soils and Waves*. John Wiley & Sons, New York (2001)

[11] H. van Olphen. *An Introduction to Clay Colloid Chemistry*. John Wiley & Sons, New York (1977)

[12] J. K. Mitchell, K. Soga. *Fundamentals of Soil Behavior*. John Wiley & Sons, Inc.(2005)

[13] I. Sogami, N. Ise. "On the electrostatic interaction in macroionic solutions" *The Journal of Chemical Physics,* 81 (1984) 6320-6332
[14] M. B. McBride, P. Baveye. "Diffuse double-layer models, long-range forces, and ordering in clay colloids" *Soil Science Society of America Journal,* 66 (2002) 1207-1217
[15] J. N. Israelachvili. *Intermolecular and Surface Forces*. Academic Press, San Diego, CA (2011)
[16] R. H. Bennett, M. H. Hulbert. *Clay Microstructure*. International Human Resources Development Corporation, Boston, MA (1986)
[17] A. C. Pierre, K. Ma. "DLVO theory and clay aggregate architectures formed with AlCl3" *Journal of the European Ceramic Society,* 19 (1999) 1615-1622
[18] A. M. Palomino, J. C. Santamarina. "Fabric map for kaolinite: Effects of pH and ionic concentration on behavior" *Clays and Clay Minerals,* 53 (2005) 209-222
[19] G. H. Bolt. "Physico-chemical analysis of the compressibility of pure clays" *Geotechnique,* 6 (1956) 86-93
[20] R. E. Olson, G. Mesri. "Mechanisms controlling compressibility of clays" *Journal of Soil Mechanics and Foundations Division, Proceedings of the American Society of Civil Engineers,* 96 (1970) 1863-1878
[21] A. Sridharan, G. V. Rao. "Mechanisms Controlling Volume Change of Saturated Clays and Role Effective Stress Concept" *Geotechnique,* 23 (1973) 359-382
[22] C. A. Moore, J. K. Mitchell. "Electromagnetic Forces and Soil Strength" *Geotechnique,* 24 (1974) 627-640
[23] A. J. Kopf, S. Kasten, J. Blees. "Geochemical evidence for groundwater-charging of slope sediments: The Nice Airport 1979 landslide and tsunami." *Submarine Mass Movements and Their Consequences*. D. C. Mosher, R. C. Shipp, L. Moscardelli, J. D. Chaytor, C. D. P. Baxter, H. J. Lee and R. Urgeles, (Eds). Springer, New York (2010) 203-214
[24] G. J. Moridis, J. Kim, M. T. Reagan, S. J. Kim. "Feasibility of gas production from a gas hydrate accumulation at the UBGH2-6 site of the Ulleung basin in the Korean East Sea" *Journal of Petroleum Science and Engineering,* 108 (2013) 180-210
[25] J. Jang, J. C. Santamarina. "Fines Classification Based on Sensitivity to Pore-Fluid Chemistry" *Journal of Geotechnical and Geoenvironmental Engineering,* 142 (2015) 06015018
[26] W. Winters, M. Walker, R. Hunter, T. Collett, R. Boswell, K. Rose, W. Waite, M. Torres, S. Patil, A. Dandekar. "Physical properties of sediment from the Mount Elbert gas hydrate stratigraphic test well, Alask North Slope" *Marine and Petroleum Geology,* 28 (2011) 361-380
[27] J. J. Bahk, D. H. Kim, J. H. Chun, B. K. Son, J. H. Kim, B. J. Ryu, M. E. Torres, M. Riedel, P. Schultheiss. "Gas hydrate occurrences and their relation to host sediment properties: Results from Second Ulleung Basin Gas Hydrate Drilling Expedition, East Sea" *Marine and Petroleum Geology,* 47 (2013) 21-29
[28] K. Egawa, O. Nishimura, S. Izumi, E. Fukami, Y. Jin, M. Kida, Y. Konno, J. Yoneda, T. Ito, K. Suzuki, Y. Nakatsuka, J. Nagao. "Bulk sediment mineralogy of gas hydrate reservoir at the East Nankai offshore production test site" *Marine and Petroleum Geology,* 66 (2015) 379-387
[29] BSI (British Standards Institution). (1990) *Methods of Test for Soils for Civil Engineering Purpose.* BS 1377, London
[30] C. P. Wroth, D. M. Wood. "The correlation of index properties with some basic engineering peroperties of soils" *Canadian Geotechnical Journal,* 15 (1978) 137-145
[31] W. D. Carrier, J. F. Beckman. "Correlations between index tests and the properties of remoulded clays" *Geotechnique,* 34 (1984) 211-228
[32] A. Sridharan, H. B. Nagaraj. "Compressibility behaviour of remoulded, fine-grained soils and correlation with index properties" *Canadian Geotechnical Journal,* 37 (2000) 712-722
[33] J. M. Lee, C. D. Shackelford, C. H. Benson, H. Y. Jo, B. E. Tuncer. "Correlating index properties and hydraulic conductivity of geosynthetic clay liners" *Journal of Geotechnical and Geoenvironmental Engineering,* 131 (2005) 1319-1329
[34] ASTM. (2011) *Standard Test Methods for One-Dimensional Consolidation Properties of Soils Using Incremental Loading.* ASTM D2435, West Conshohocken, PA
[35] J. C. Santamarina, K. A. Klein, Y. H. Wang, E. Prencke. "Specifice surface: determination and relevance" *Canadian Geotechnical Journal,* 39 (2002) 233-241
[36] R. Arnott. "Particle sizes of clay minerals by small-angle X-ray scattering" *The American Mineralogist,* 50 (1965) 1563-1575
[37] W. Ducker, T. J. Senden, R. M. Pashley. "Direct measurement of colloidal forces using an atomic force microscope" *Letters to Nature,* 353 (1991) 239-241
[38] Y. J. Yang, A. V. Kelkar, D. S. Corti, E. I. Franses. "Effect of Interparticle Interactions on Agglomeration and Sedimentation Rates of Colloidal Silica Microspheres" *Langmuir,* 32 (2016) 5111-5123

[39] B. Tiwari, B. Ajmera. "Consolidation and swelling behavior of major clay minerals and their mixtures" *Applied Clay Science,* 54 (2011) 264-273
[40] H. K. Kim, J. Santamarina. "Sand-rubber mixtures (large rubber chips)" *Canadian Geotechnical Journal,* 45 (2008) 1457-1466
[41] R. K. Taylor, T. J. Smith. "The engineering geology of clay minerals: Swelling, shrinking and mudrock breakdown" *Clay Minerals,* 21 (1986) 235-260